CHEMICAL ENGINEERING TRANSACTIONS
VOL. 74, 2019
A publication of AIDIC
The Italian Association of Chemical Engineering
Online at www.cetjournal.it
Guest Editors: Sauro Pierucci, Jiří Jaromír Klemeš, Laura Piazza

ISBN 978-88-95608-71-6; **ISSN** 2283-9216
DOI: 10.3303/CET1974153

Liquid Flow Morphology of Viscous Systems in Structured Packings: Investigations by X-ray Tomography

Lukas Bolenz[a], Dominique Toye[b], Eugeny Y. Kenig[a,*]

[a]Chair of Fluid Process Engineering, Paderborn University, Pohlweg 55, 33098 Paderborn, Germany
[b]Department of Chemical Engineering, University of Liège, Allée de la chimie, B6C, Sart Tilman, 4000 Liège, Belgium
eugeny.kenig@uni-paderborn.de

In the modeling of gas-liquid separation processes in structured packings, fluid dynamics is often reduced to a uniform liquid film flow over the packing surface. However, previous experiments with X-ray tomography indicate that this assumption is not valid when the liquid-phase viscosity is significantly higher than 1 mPa s. In order to improve existing modeling approaches for viscous systems, a better understanding of the influence of the liquid viscosity on the liquid flow inside the structured packing is necessary. In this work, X-ray tomography is used to investigate the flow morphology of liquid systems with low surface tension and a viscosity up to 50 mPa s. An empirical correlation that describes the hold-up fraction of the existing flow patterns is given and a modelling approach is proposed that allows to consider the influence of the different flow patterns on mass transfer.

1. Introduction

In gas-liquid separation processes, structured packings are widely used as column internals, since they provide good separation performance combined with a relatively low pressure drop. Modelling approaches for the prediction of fluid dynamics as well as heat and mass transfer in such internals have been suggested which often assume a uniform liquid film flow on the packing surface (Rocha et al., 1993; Shilkin and Kenig, 2005).
For the analysis of the real flow behavior in structured packings, X-ray tomography offers a non-invasive method. It has been used for the determination of liquid hold-up and gas-liquid interfacial area of air-water systems in catalytic packings as well as high-performance packings (Aferka et al., 2010a,b, 2011; Viva et al., 2011). Schug and Arlt (2016) analyzed the film thickness on the packing surface by high-resolution X-ray tomography and showed that the equation derived from the simplified Nusselt theory of laminar film yields significantly underestimated values. Wehrli et al. (2018) employed X-ray tomography to compare axial hold-up profiles of aqueous and non-aqueous systems and found no qualitative difference. Janzen et al. (2013) used a water-glycerol mixtures with varying viscosity of the liquid phase up to 20 mPa s. Along with investigation of hold-up and interfacial area, they quantified the different flow patterns that arise inside the structured packing. For hold-up, interfacial area and the hold-up fraction of individual flow patterns, an influence of the viscosity could be observed. In particular, the fraction of the film flow decreased below 60%, thus indicating that the assumption of a uniform liquid flow is not valid for higher viscosities.
In the present study, further investigations on the fluid dynamics of viscous systems in structured packings are carried out. Here, the viscosity of the liquid phase is increased to the maximum of 50 mPa s and the surface tension of the water-glycerol mixture is reduced by a surfactant in order to mimic the wetting behavior of non-aqueous systems. The occurrence of flow patterns other than film flow likely has an impact on mass transfer performance. However, this has not been considered in existing modeling approaches yet. Based on geometrical consideration, an approach is presented that allows the influence of different flow patterns to be taken into account.

Paper Received: 4 May 2018; Revised: 29 October 2018; Accepted: 26 January 2019

Please cite this article as: Bolenz L., Toye D., Kenig E., 2019, Liquid Flow Morphology of Viscous Systems in Structured Packings: Investigations by X-ray Tomography, Chemical Engineering Transactions, 74, 913-918 DOI:10.3303/CET1974153

2. Material and methods

2.1 Experimental setup

The experiments are carried out with a high energy (420 kV) X-ray tomograph (Figure 1). A rotating column with a diameter of 100 mm is installed between the X-ray source and the detector. The column is equipped with four structured packing elements of Mellapak 350.Y, each with a 200 mm height, that are rotated 90° with respect to each other. Between the elements and a multiple point source distributor (4000 drip points/m²) at the top of the column, a bed of random packings (Pall rings) is placed to obtain a uniform liquid distribution. At the bottom of the column, the liquid is collected in a tank and continuously pumped back to the column top in order to maintain a constant liquid flow. Further details on the experimental setup are given by Toye et al. (2005).

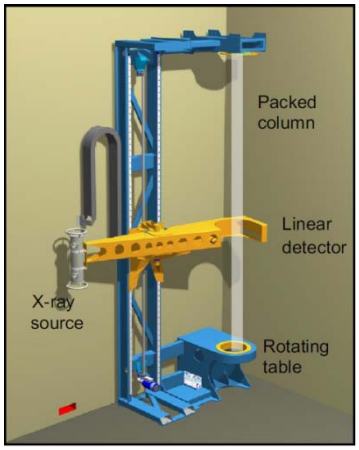

Figure 1: X-ray tomography facilities (cf. Aferka et al., 2011)

2.2 Chemical system

A mixture of water and glycerol is used as the working liquid, which has been successfully applied in previous studies (Janzen et al., 2013) and allows an accurate adjustment of the liquid viscosity. In order to mimic the wetting behavior of non-aqueous systems with significantly lower surface tension, a surfactant (Ethylan 1003 supplied by AkzoNobel) is added to the mixture which reduces the surface tension to a minimum of approx. 29 mN/m. This value is reached when the surfactant concentration at the gas-liquid interface is in equilibrium. Measurements of surface tension performed for different viscosity values show that the influence of viscosity or, in other words, composition of the mixture on the surface tension can be neglected. Furthermore, an anti-foaming agent (Entschäumer 1833 supplied by EFA Chemie GmbH) is used to minimize the foam formation due to the surfactant. The liquid mixture compositions for different viscosities are given in Table 1.

Table 1: Weight fractions of the components in the liquid mixture for the analysed viscosities

	5 mPa s	20 mPa s	35 mPa s	50 mPa s
Water	0.5280	0.3113	0.2481	0.2125
Glycerol	0.4609	0.6772	0.7403	0.7758
Surfactant	0.0100	0.0100	0.0100	0.0100
Anti-foaming agent	0.0011	0.0015	0.0016	0.0017

2.3 Experimental procedure

First, tomographic measurements of the dry column are carried out in order to obtain data of the non-irrigated packings that are necessary for the later image reconstruction and post-processing. Different column cross-sections are scanned subsequently in a 10 mm distance over almost the whole length of the structured packing section. Afterwards, the measurements are repeated at exactly the same positons for the irrigated column. For each viscosity (5, 20, 35 and 50 mPa s), four different liquid loads (5, 10, 15 and 20 m³/(m²/h)) and a countercurrent air flow with a constant F-factor of 2 $Pa^{0.5}$ are applied.

2.4 Image reconstruction and post-processing

To obtain images of the liquid distribution in a column cross-section, the projection data of the dry column is subtracted from the data of the irrigated column. A classical linear back projection algorithm implemented in

the Fourier domain and adapted to the fan beam geometry (see Kak and Slaney, 1988) is applied, resulting in grayscale images of 499 x 499 pixels with a spatial resolution of 0.36 x 0.36 mm. Afterwards, the background noise is eliminated by evaluating a threshold value with Otsu's method (Otsu, 1979). Further information on the image reconstruction and post-processing can be found in Aferka et al. (2007) and Viva et al. (2011).

2.5 Liquid hold-up determination

For the determination of the liquid hold-up, it is assumed that a white pixel represents a volume element that is completely filled with air while a volume element represented by a black pixel is completely filled with water. A volume element containing both air and water is represented by a gray pixel with the gray value corresponding to the amount of water inside this section. Thus, the hold-up, defined as the fraction of water in the column cross-section, can be calculated from the gray values of all pixels belonging to the cross-section image. Details of this procedure are given by Aferka et al. (2010).

2.6 Identification of liquid flow pattern

Janzen et al. (2013) developed an analysis algorithm to quantify the hold-up fraction of different liquid flow patterns in tomographic images based on geometric considerations. Each flow pattern has a specific size and shape. Two different flow patterns that could be observed within the present work are film flow and contact-point (C-P) liquid. The latter represents the accumulation of liquid at contact points between two adjacent packing sheets. Film flow on the packing surface is identified with a thin and elongated structure, whereas C-P liquid is rather small and compact. To determine the shape of a pixel structure, the Feret diameters of the structure are used. The Feret diameter is a parameter that is originally used in particle technology and defined as the distance between two parallel tangents of the particle projection area. The minimum F_{min} and maximum F_{max} Feret diameters are estimated for all pixel structures as well as the total pixel area A_i determined as the number of pixels belonging to a structure times the area of a single pixel. Each pixel structure is evaluated by means of the criteria given in Table 2, which were slightly changed compared to Janzen et al. (2013) to account for the different packing geometry. If at least one criterion is met, the pixel structure is identified as C-P liquid. Pixel structures that cannot be identified as C-P liquid are assigned to film flow.

Table 2: Criteria for the assignment of C-P liquid to pixel structures

Flow pattern	Criterion 1	Criterion 2
C-P liquid	$\frac{F_{max}}{F_{min}} < 2 \;\&\; F_{min} \geq 7\ \mathrm{mm}$	$\frac{F_{max}}{F_{min}} \geq 2 \;\&\; F_{min} > 8.8\ \mathrm{mm} \;\&\; \frac{A_i}{F_{max}\,F_{min}} > 0.5$

2.7 Calculation of the surface-to-volume ratio

Interphase mass transfer takes places at the interface of two phases. In gas-liquid separation processes, mass transfer acceleration is desirable, which requires a large gas-liquid interface. To evaluate the influence of different flow patterns on mass transport, a simple approach is used to calculate the average surface-to-volume ratio of each flow pattern.

As describe above, it is possible to assign a pixel within a tomographic image representing the liquid phase to a specific flow structure. Subsequently, the direct neighbors of this pixel are analyzed whether they are associated to air or liquid. If one or more of these are associated to air, the original pixel is assigned to the surface of the pixel structure. Finally, the average surface-to-volume ratio of a flow pattern is determined as the ratio of surface pixels and the total number of pixels belonging to this flow pattern.

3. Results and discussion

3.1 Liquid hold-up

Figure 2 exemplarily shows the axial profiles of the liquid hold-up for different liquid loads at a viscosity of η = 35 mPa s. As expected, the hold-up increases with higher liquid loads. However, at the intersection between the packing elements (dashed lines) a significant decrease in the hold-up can be seen. In the previous studies (Aferka et al., 2010; Viva et al., 2011; Janzen et al., 2013), a similar qualitative behavior appeared only in high- performance packings with a vertical corrugation and hence high liquid-phase velocities at the packing edges, whereas for conventional packings, even a hold-up increase was detected (Green et al., 2007; Schug and Arlt, 2016). In the present work, it was found that at the intersections between two packing elements, the cross-section of the upper element contains a relatively large portion of liquid and that the decrease appears in the top cross-section of the lower element. Due to the 90° rotation of the lower element with respect to the upper element, the liquid cannot continue flowing along the packing surface when it

reaches the intersection and drips from the edge. This effect is reinforced through the low surface tension of the liquid phase. The falling liquid has a relatively high velocity, which leads to a shorter residence time in the respective packing layer and thus to a lower local hold-up.

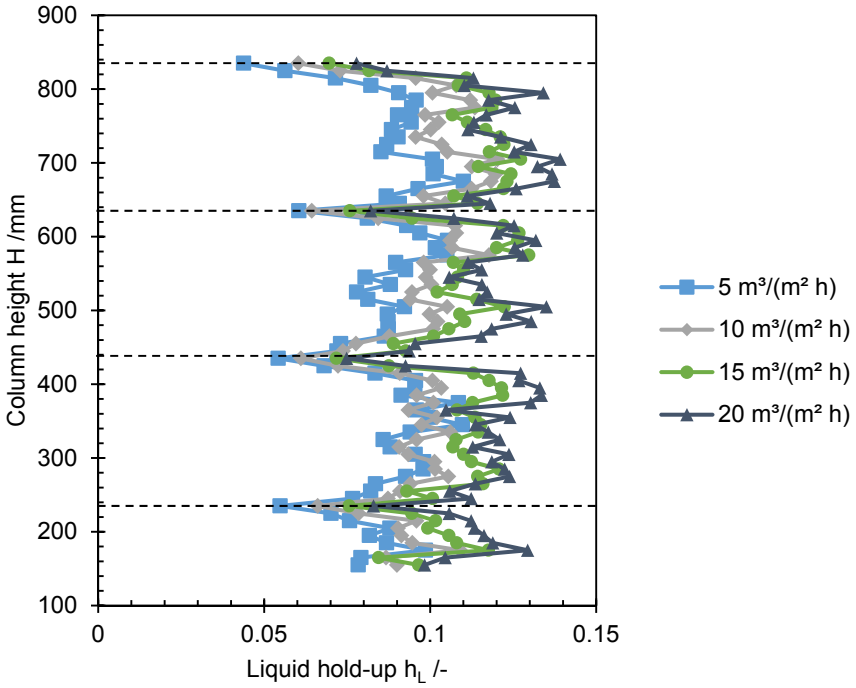

Figure 2: Axial profiles of the liquid hold-up for different liquid loads and a viscosity of η = 35 mPa s

3.2 Liquid flow morphology

The tomographic images were analyzed with respect to the liquid flow patterns. A typical image of the liquid distribution inside a cross-section is shown in Figure 3. The dominant flow pattern is the film flow, which can be easily recognized in the image, as it follows the geometry of the structured packing. Furthermore, at the contact points of the adjacent packing sheets C-P liquid is visible. In contrast to the previous work (Janzen et al., 2013), no completely flooded channels can be detected. Due to the larger channel size in the Mellapak 350.Y packing compared to the Mellapak 752.Y used by Janzen et al. (2013) and because of the lower surface tension of the liquid phase, the occurrence of flooded channels is less likely.

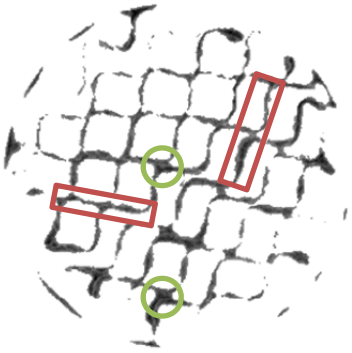

Figure 3: Flow patterns inside a packing cross-section: red rectangles - film flow, green circles - C-P liquid

The method presented in Section 2.6 allows quantification of the relative contribution of individual flow patterns to the liquid hold-up. Figure 4 shows for different liquid loads how the film-flow fraction changes with viscosity. Since in this work only two flow patterns, film flow and C-P liquid, are discriminated, the fraction of the latter pattern can directly be derived from the values of the first one. For a low viscosity of 5 mPa s, the fraction of the film flow is close to one and C-P liquid pattern can be nearly neglected. For higher viscosities, the film-flow fraction significantly decreases down to values between 0.8 and 0.9, while the decrease is steeper for higher liquid loads. Both higher viscosities and higher liquid loads result in thicker liquid films on the packing sheets and thus promoting the formation of C-P liquid.

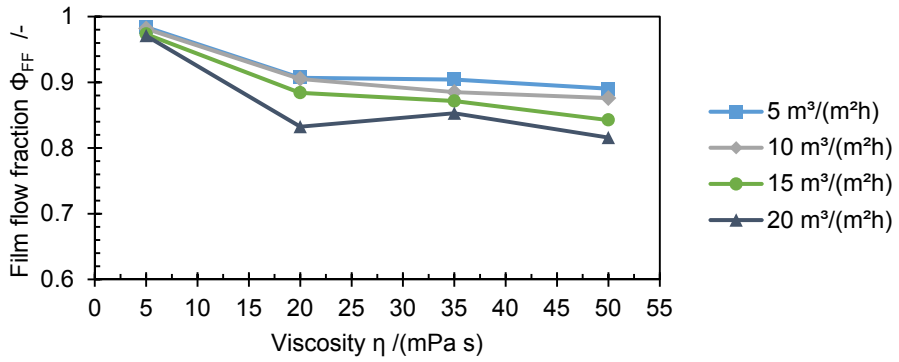

Figure 4: Film-flow fraction of the total liquid hold-up for varying viscosities and liquid loads

To evaluate the fractions of individual flow patterns as functions of liquid viscosity and liquid load, an empirical correlation was derived based on 1104 data points. For both determining factors, a linear correlation was assumed. The equation resulting from multiple linear regression is as follows:

$$\Phi_{FF}=1.010 - 0.0024\ \eta - 0.0036\ L \quad (1)$$

where Φ_{FF} is the dimensionless hold-up fraction of the film flow, η is viscosity in mPa s and L is liquid load in m³/(m² h). The coefficient of determination (R^2-value) for this regression is 0.773.

3.3 Surface-to-volume ratios

For each operating point, the average surface-to-volume ratio was evaluated for film flow and for C-P liquid. Figure 5a shows exemplarily the values for a liquid load of 15 m³/(m² h) varying between 0.75 and 0.9 m²/m³ for film flow and between 0.4 and 0.5 m²/m³ for C-P liquid. Furthermore, the ratio of C-P liquid is divided through the ratio of film flow for each operating point. As can be seen in Figure 5b, C-P liquid has a surface-to-volume ratio that ranges between 50 and 65% of the film flow. Furthermore, a certain influence of viscosity and liquid load on the ratio is visible. Increasing viscosity and increasing liquid load lead to even larger difference between the two flow patterns. Due to the elongated shape of the film-flow structure, thicker liquid films effect the surface-to-volume ratio less significantly than the rather compact C-P liquid patterns.

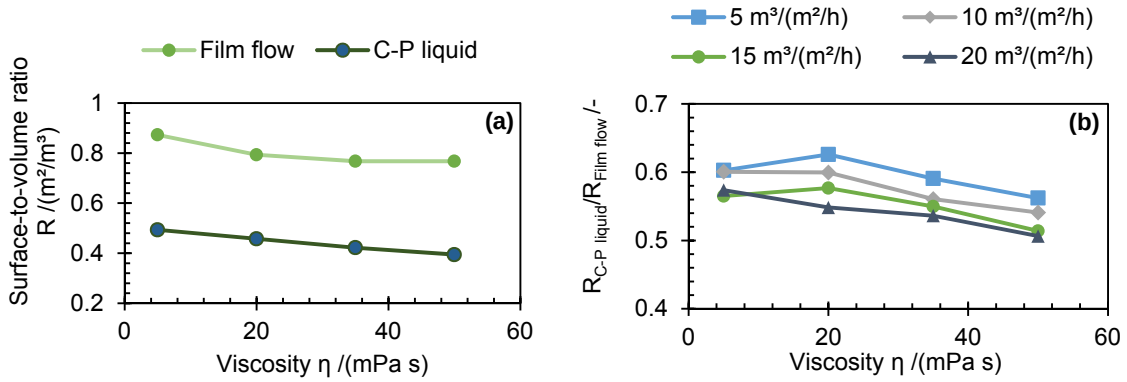

Figure 5: The surface-to-volume ratio of film flow and C-P liquid for a liquid load of 15 m³/(m² h) and varying viscosity (a); the surface-to-volume ratio of CP-liquid $R_{C\text{-}P\ liquid}$ in relation to film flow $R_{Film\ flow}$ for varying liquid loads and viscosities (b)

4. Conclusions

Tomographic experiments were carried out to investigate the influence of the liquid viscosity on the fluid dynamics in structured packings. Axial profiles of the liquid hold-up show an unexpected decrease at the transition between two packing elements that can be explained with the low surface tension of the liquid. The analysis of the flow morphology shows that for low viscosities, the film-flow fraction is slightly below 100% and decreases up to values of approx. 80% for a viscosity of 50 mPa s. An empirical correlation describing the film-flow hold-up fractions as a function of viscosity and liquid load was derived using multiple linear regression. The surface-to-volume ratio was introduced as an important parameter for the evaluation of the influence of different flow structures on the mass transfer. It was found that the surface-to-volume ratio for C-P liquid amounts to 50 - 65% of the values for the film flow.

Acknowledgments

We are grateful to Deutsche Forschungsgemeinschaft (DFG) for the financial support (project KE 837/19-3) and to Sulzer AG for providing the structured packings.

References

Aferka, S., Crine, M., Saroha, A.K., Toye, D., Marchot, P., 2007, In situ measurements of the static liquid holdup in Katapak- SP12TM packed column using X-ray tomography, Chemical Engineering Science, 62, 6076-6080.

Aferka, S., Marchot, P., Crine, M., Toye, D., 2010a, Interfacial area measurement in a catalytic distillation packing using high energy X-ray CT, Chemical Engineering Science, 65, 511-516.

Aferka, S., Viva, A., Brunazzi, E., Marchot, P., Crine, M., Toye, D., 2010b, Liquid load point determination in a reactive distillation packing by X-ray tomography, The Canadian Journal of Chemical Engineering, 62, 611-617.

Aferka, S., Viva, A., Brunazzi, E., Marchot, P., Crine, M., Toye, D., 2011, Tomographic measurement of liquid hold up and effective interfacial area distributions in a column packed with high performance structured packings, Chemical Engineering Science, 66, 3413-3422.

Green, C.W., Farone, J., Briley, J.K., Eldridge, R.B., Ketcham, R.A., Nightingale, B., 2007, Novel Application of X-ray Computed Tomography: Determination of Gas/Liquid Contact Area and Liquid Holdup in Structured Packing, Industrial & Engineering Chemistry Research, 46, 5734-5753.

Janzen, A., Steube, J., Aferka, S., Kenig, E.Y., Crine, M., Marchot, P., Toye, D., 2013, Investigation of liquid flow morphology inside a structured packing using X-ray tomography, Chemical Engineering Science, 102, 451-460.

Kak, A.C., Slaney, M., 1988, Principles of computerized tomographic imaging, IEEE Press, New York, USA.

Otsu, N., 1979, A Threshold Selection Method from Gray-Level Histograms, IEEE Transactions on Systems, Man, and Cybernetics, 9, 62-66.

Rocha, J.A., Bravo, J.L., Fair, J.R., 1993, Distillation columns containing structured packings: a comprehensive model for their performance. 1. Hydraulic models, Industrial & Engineering Chemistry Research, 32, 641-651.

Schug, S., Arlt, W., 2016, Imaging of Fluid Dynamics in a Structured Packing Using X-ray Computed Tomography, Chemical Engineering & Technology, 39, 1561-1569.

Shilkin, A., Kenig, E.Y., 2005, A new approach to fluid separation modelling in the columns equipped with structured packings, Chemical Engineering Journal, 110, 87-100.

Toye, D., Crine, M., Marchot, P., 2005, Imaging of liquid distribution in reactive distillation packings with a new high-energy x-ray tomograph, Measurement Science and Technology, 16, 2213-2220.

Viva, A., Aferka, S., Brunazzi, E., Marchot, P., Crine, M., Toye, D., 2011, Processing of X-ray tomographic images: A procedure adapted for the analysis of phase distribution in MellapakPlus 752.Y and Katapak-SP packings, Flow Measurement and Instrumentation, 22, 279-290.

Wehrli, M., Kögl, T., Lindner, T., Arlt, W., 2018, An unobstructed view of liquid flow in structured packing, Chemical Engineering Transactions, 69, 775-780.